



**HAL**  
open science

# Experimental investigation of performance, emission and combustion characteristics of olive mill wastewater biofuel blends fuelled CI engine

Loubna Hadhoum, Fatma Zohra Aklouche, Khaled Loubar, Mohand Tazerout

## ► To cite this version:

Loubna Hadhoum, Fatma Zohra Aklouche, Khaled Loubar, Mohand Tazerout. Experimental investigation of performance, emission and combustion characteristics of olive mill wastewater biofuel blends fuelled CI engine. *Fuel*, 2021, 291, pp.120199. 10.1016/j.fuel.2021.120199 . hal-04660879

**HAL Id: hal-04660879**

**<https://hal.science/hal-04660879v1>**

Submitted on 13 Nov 2024

**HAL** is a multi-disciplinary open access archive for the deposit and dissemination of scientific research documents, whether they are published or not. The documents may come from teaching and research institutions in France or abroad, or from public or private research centers.

L'archive ouverte pluridisciplinaire **HAL**, est destinée au dépôt et à la diffusion de documents scientifiques de niveau recherche, publiés ou non, émanant des établissements d'enseignement et de recherche français ou étrangers, des laboratoires publics ou privés.



Distributed under a Creative Commons Attribution - NonCommercial 4.0 International License

# 1           **Experimental investigation of performance, emission and** 2           **combustion characteristics of olive mill wastewater biofuel blends** 3           **fuelled CI engine**

4           *Loubna HADHOUM, Fatma Zohra AKLOUCHE, Khaled LOUBAR\*, and Mohand*  
5           *TAZEROUT*

6           *IMT Atlantique, Energy Systems and Environment Department, GEPEA, UMR CNRS 6144,*  
7           *04 rue Alfred Kastler, CS 20722, 44307 Nantes Cedex 3, France.*

8           \*Corresponding author: [Khaled.loubar@imt-atlantique.fr](mailto:Khaled.loubar@imt-atlantique.fr) (ORCID: 0000-0003-1578-6475)

## 9           **ABSTRACT**

10          The current study investigates the opportunity of using olive mill wastewater (OMWW) as a  
11          renewable fuel in internal combustion engines. The biofuel was made from the hydrothermal  
12          conversion of OMWW using sub-/supercritical alcohol-water system. OMWW biofuel was blended  
13          with pure diesel (designated B0). Three blends namely B10, B20 and B30 containing respectively  
14          10%, 20% and 30% by volume of biofuel were tested. This paper focuses on the experimental study of  
15          the performance, combustion and emission characteristics of a diesel engine using OMWW biofuel as  
16          a partial replacement of conventional diesel fuel. All experiments were performed with constant  
17          engine speed (1500 rpm). The engine load was varied from 20 to 100% of full load. It is found that  
18          B10 blend offers the best results, compared to B20 and B30, in terms of performance and pollutant  
19          emissions. Using B10 showed lower emission levels for unburned hydrocarbons (12%), particulate  
20          matter (12%) and carbon monoxide (26%) under high load conditions, compared to that of  
21          B20. Moreover, under medium load conditions, B10 further reduced the concentration of pollutants  
22          such as particulate matter (55%) and carbon monoxide (65%) compared to that of B30. In addition, the  
23          use of B20 and B30 blends resulted in a lower thermal efficiency than that of diesel fuel. Conversely,  
24          the thermal efficiency obtained with B10 was the highest even compared to diesel fuel.

25          **Keywords:** Biofuel-diesel blend; Emission; alcohol; olive mill wastewater; diesel engine.

27

28 **Nomenclature**

$Q$	heat, [J]
$\gamma$	Ratio of specific heats, [-]
$P$	Cylinder pressure, [bar]
$P_{out}$	Brake power output, [kW]
$V$	Cylinder volume, [m <sup>3</sup> ]
BTE	Brake thermal efficiency, [%]
BSFC	Brake specific fuel consumption [g/kWh]
LHV	Lower calorific value, [MJ/kg]
$\dot{m}$	Mass flow rate, [kg/s]
ID	Ignition delay, [deg CA]
$\theta$	Crank angle, [deg CA]
$L$	Connecting rod length, [m]
$V_d$	Displacement volume, [m <sup>3</sup> ]
$C$	Stroke, [m]
CA	Crank angle
Cr	Compression ratio
PDP	Physical delay period
CDP	Chemical delay period
$\phi$	Equivalence ratio
TDC	Top dead center
CI	Compression ignition
HC	Hydrocarbon
NO <sub>x</sub>	Nitrogen oxides
CO <sub>2</sub>	Carbon dioxide
CO	Carbon monoxide
OMWW	Olive mill waste water
HTL	Hydrothermal liquefaction
HRR	Heat release rate

29

30

31

32

33

34

35

36

## 37 **1. Introduction**

38 Nowadays, the world is facing a fossil fuel depletion crisis and environmental degradation due to  
39 the pollution from transportation sector. The reduction in underground carbon resources is due to  
40 excessive consumption and the indiscriminate extraction of fossil fuels [1]. Adverse effects on human  
41 health such as respiratory, development of cancer, cardiovascular diseases, are caused by exhaust gas  
42 emissions of internal combustion (IC) engine [2]. In addition, fossil fuels face other challenges, such  
43 as the limited capacity of refineries, depletion of resources and security of supply. The search for  
44 alternative renewable fuels has become highly pronounced in the current context, promising a  
45 harmonious relation with environmental preservation, management, efficiency, energy conservation,  
46 and sustainable development. Therefore, it is important to accelerate the development and the use of  
47 new alternative energy sources by developing energy efficiency and economical processes for the  
48 production of fuels and chemicals [3]. The alternative fuel must be technically feasible, economically  
49 competitive and easily available. [4].

50  
51 Recently, biofuels produced from renewable resources such as plants or biomass-derived organic  
52 waste, have become more attractive due to their various benefits, which are related to economy,  
53 environment and energy security. Among the major advantages of biofuels: (i) the availability from  
54 various biomass sources, (ii) they have a considerable environmentally friendly potential, and allow  
55 reduction in greenhouse gases, (iii) they are biodegradable and contribute to the sustainability [5]. The  
56 production of biofuels is evolving from a range of sources. First generation biofuels are produced from  
57 foods and agriculture resources [6]. Second generation biofuels, on the other hand, are produced from  
58 non-food biomass sources [7]. The structured fraction of biomass feedstock is typically composed  
59 from hemicelluloses, cellulose and lignin. In addition, the early focus among second generation liquid  
60 biofuel (e.g. bio-oil, biobutanol, bioethanol and biodiesel) researchers and producers was often on the  
61 lignocellulosic inedible biomass. Therefore, the use of second generation feedstock, which includes  
62 inedible and waste, is considered as potential alternative fuel source.

63 Many conversion processes are currently available and well established for the production of  
64 transport biofuels from different types of biomass, including esterification, fermentation, digestion,

65 hydrothermal liquefaction (HTL), gasification and thermal cracking (pyrolysis) [8]. Among  
66 thermochemical conversion processes, recently HTL has attracted much attention due to the direct use  
67 of biomass without the need for a preliminary drying step [9]. HTL process aims to produce low  
68 molecular weight liquids from a high organic molecular weight feedstock under subcritical or  
69 supercritical conditions. The processing of biomass is carried out at moderate temperature and  
70 pressure typically between 250-350°C and 10-20MPa, respectively, in the absence of oxygen [10]. The  
71 liquefaction products are generally biofuel fraction, aqueous phase, solid residues and a CO<sub>2</sub>-rich gas  
72 fraction. The biofuel produced has a high calorific value in the range of 30-43 MJ/kg [11-13], and  
73 lower oxygen content compared with biofuel from pyrolysis process. Therefore, the HTL biofuel has  
74 suitable properties to be used as engine fuel [14].

75

76 On the other hand, olive oil consumption is rapidly increasing worldwide, due to its high dietetic  
77 and nutritional value. The three major olive oil producers worldwide are Italy, Spain and Greece,  
78 followed by Turkey, Tunisia, and to a lesser extent Portugal, Morocco, and Algeria [15]. The  
79 traditional press extraction method as well as the continuous three-phase decanter process, which is  
80 most widely used for the production of olive oil, generate three products: olive oil, olive husk and  
81 aqueous waste called olive mill wastewater (OMWW). A serious ecological problem represented by  
82 the treatment of OMWW due to its high degree of organic pollution and its pH slightly acid [16,17].  
83 Regarding the environmental impact, it is considered to be a significant polluting waste in all  
84 Mediterranean regions [18]. Indeed, in terms of pollution effect, 1 m<sup>3</sup> of OMWW is equivalent to 100-  
85 200 m<sup>3</sup> of domestic sewage [15]. Its uncontrolled disposal in water reservoirs leads to severe problems  
86 for the whole ecosystem and especially for the natural water bodies (ground water reservoirs, surface  
87 aquatic reservoirs, seashores, and sea). It is a turbid liquid, black to dark brown in colour and smells of  
88 oil [16,19]. In addition, the dark colour of this waste depends on the age, olive type processed as well  
89 as the technology used to extract oil. Its characteristics are very variable and depend on many factors  
90 such as the variety and maturity of the olives, the employed extraction technology, the climatic  
91 conditions, the cultivation management and the storage time [16,19]. OMWW can be considered as a  
92 serious option to produce biofuel since it is inedible and a non-food feedstock.

93 Few research studies dealing with the strategy adopted to recover these waste through the  
94 thermochemical conversion are available. Pyrolysis of OMWW on dried samples has been thoroughly  
95 investigated at a heating rate of 5°C/min in order to study the gas formation during this process [20].  
96 Nevertheless, using pyrolysis process is not suitable for this kind of waste due to its high moisture  
97 content (more than 80%) [21]. Miranda et al. [22] investigated the combustion of OMWW by  
98 studying the thermal behaviour of different wastes coming from olive oil mills by using the  
99 thermogravimetric techniques in oxidizing atmosphere. Moreover, Ekin et al [23] examined the  
100 gasification of the liquid waste from industrial olive oil in supercritical water. The maximum amount  
101 of gas produced, which was 7.7 ml per ml of OMWW, was observed at reaction temperature of 550°C,  
102 with a reaction time of 30s. On the other hand, the hydrothermal carbonization of OMWW was  
103 studied by Poerschmann et al [24]. They reported that the bio-char yield of 30% (w/w) was associated  
104 to the low carbohydrate fraction in the OMWW but no information regarding the bio-oil was  
105 published. According to literature, conversion of OMWW into bio-oil, via hydrothermal liquefaction,  
106 was considered recently in two studies using sub- and supercritical in water and alcohols [14,21]. They  
107 found a bio-oil viscosity of 10.2 and 7.6 mPa.s using ethanol- water and methanol-water co-solvent,  
108 respectively. The higher heating value of 43.20 MJ/kg was obtained employing MeOH-water co-  
109 solvent which resulted in better physical and chemical properties.

110

111 Regarding the use of biofuel in compression ignition (CI) engines, the literature shows a  
112 variety of aspects in order to enhance the combustion parameters and engine performance [25–28].  
113 Most of these researches focused on the use of biodiesels and diesel-biodiesel blends. Indeed, biofuels  
114 can be blended with neat diesel in any proportion to obtain a biofuel blend, leading to lower  
115 hazardous exhaust emissions, resulting in unchanged or improved engine efficiency [29,30]. Table 1  
116 presents some literature studies about the impact of different blends on engine performance from  
117 various biofuel sources. Recently algae biodiesel blended in two different proportions (10% and 15%)  
118 with diesel, was investigated by Indrareddy et al. [31] on a common rail direct injection diesel engine.  
119 The study reported that for both blends, carbon monoxide (CO) exhibits the maximum reduction  
120 compared to diesel. The authors concluded that B15 blend can be used as an alternative fuel in the

121 diesel engine. Moreover, high injection pressures, i.e. 1050 bar, show a considerable improvement in  
 122 performance and emission characteristics. Miraculas, G. A et al. [32], have studied the performance of  
 123 biofuel from *Calophyllum inophyllum* oil-based methyl ester and its blends (0, 20, 40, 60 and 100%)  
 124 with diesel on internal combustion engines. The results were analysed statistically using an  
 125 experimental design. It was reported that the designed empirical statistical model for optimum  
 126 performance with lower emission is found to be B30, resulting in a lower break specific fuel  
 127 consumption at higher loads compared to that of diesel and led to lower emissions. On the other hand,  
 128 Chauhan, B. S et al. [33] made a review of the effect on performance and emissions of biofuel blends  
 129 from different renewable sources. The review reports that, based on combustion and performance  
 130 characteristics, biodiesel-diesel blends containing about 10–20% showed better results than higher  
 131 blends. However, the use of these blends in diesel engine causes an increase in NO<sub>x</sub> emission and a  
 132 decrease in HC, CO and PM emissions compared to diesel.

133

134 **Table 1.** Literature review of biofuels from different sources and the impact of different blends on  
 135 engine performance.

Feedstock source	Process of biofuel production	Engine loads (biofuel-diesel blends)	Remarks	Ref
<i>Calophyllum inophyllum</i> oil	Esterification	0, 20, 40, 60 and 100%	-Lower emissions were recorded for B30 at a compression ratio (CR) of 19. - The NO <sub>x</sub> emission increases with CR for higher biofuel blends but reduces the CO and HC emission than that of original CR at maximum load.	[32]
<i>Crude Karanja Oil</i>	Transesterification	10, 20, 30, 40, 50, 80 and 100%	- Brake thermal efficiencies (BTE) of blends have been found to be on increasing trend up to 70% as the load increases. B50 and B100 showed a low brake thermal efficiency.	[27]
Need seeds	Pyrolysis	5% and 10%	- A decrease in BTE till low load and increases in full load along with the reduction in HC, CO, CO <sub>2</sub> , and NO <sub>x</sub> at full load conditions were noticed.	[34]
Australian pinus radiata wood flour	Hydrothermal liquefaction	5%, 10% and 20%	- With 20% biodiesel, the properties are almost equal to that of diesel but a decrease of engine performance and increase of NO <sub>x</sub> emissions are noticed. -A maximum of 33% reduction in particulate matter (PM) emissions was observed with 20% blend	[34]
<i>Pistacia lentiscus</i> seed	Liquefaction	30 and 50%	- 50% of blend results in a considerable low NO <sub>x</sub> emissions level as compared with neat diesel fuel	[35]

136 The literature survey reveals that the usage of biodiesels, obtained from vegetable oils and animal fats,  
137 in CI engines are widely examined. In fact, biodiesels must meet the international standards and  
138 therefore their characteristics are not that different. However, few works investigated the use of  
139 alternative fuels, obtained from wastes via HTL, in engine as the biofuel characteristics could be  
140 different from that of conventional diesel. This constitute our motivation to make biofuel from HTL of  
141 OMWW. The focus of this research is to analyse and evaluate the effects of diesel and biofuel blend  
142 on diesel engine performance and emission characteristics under various loads. For that, the  
143 physicochemical properties of biofuel and biofuel blends are determined according to the standard  
144 methods and compared with those of conventional diesel fuel. Thereafter, an experimental  
145 investigation is carried out to study the effect of this biofuel blended with diesel fuel (10, 20 and 30%  
146 by v.) on the performance and the exhaust emissions (carbon monoxide CO, unburned hydrocarbon  
147 HC, nitrogen oxide NO<sub>x</sub> and soot) of a diesel engine operating under various engine load conditions.  
148 Results are compared with those of conventional diesel operation, taken as a baseline. To the best of  
149 our knowledge, there is no study dealing with the use of blended biofuel from HTL of OMWW in a  
150 conventional diesel engine.

## 151 **2. Materials and methods**

### 152 **2.1. Bio-fuel production**

153 The OMWW feedstock used to produce biofuel was collected from a traditional oil mill in Beni  
154 Amrane, a city situated in the north of Algeria. The characteristics of the feedstock (i.e. ash content,  
155 water content, volatile matter, fixed carbon, fat and the C, H, N contents) were determined using the  
156 protocols reported in the previous work [36]. The biofuel was produced using a HTL batch reactor at  
157 high temperature (200-320°C) and pressure (5-17 MPa) in the oxygen absence. Nitrogen was used to  
158 sweep air from the reactor inside before heating start. Ethanol co-solvent with a ratio of 50/50% was  
159 used as alcohol to upgrade the quality of biofuel as reported in our previous work [14]. The schematic  
160 of biofuel production from OMWW liquefaction is illustrated in Figure 1.



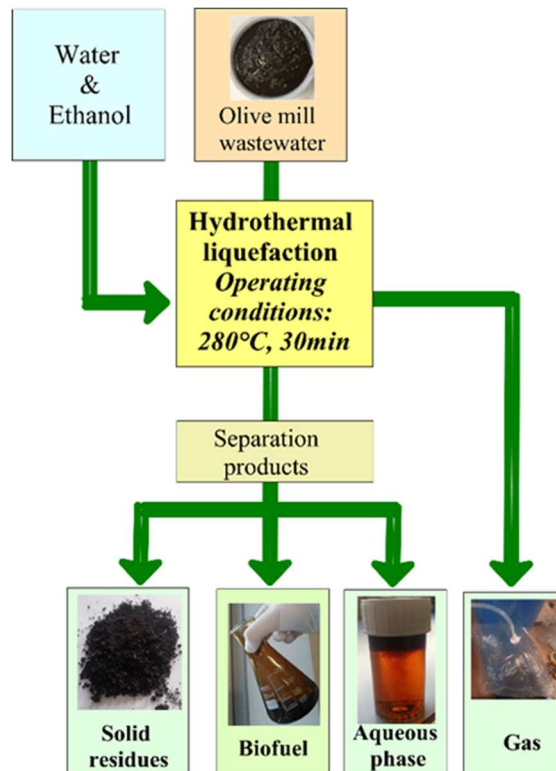


**Fig.1.** Schematic presentation of biofuel production.

## 2.2. Biofuel properties

The main physical and chemical properties of biofuel blends and diesel were determined according to ASTM standard and are depicted in Table 2. The biofuel obtained from the liquefaction of OMWW is composed of a large quantity of esters, about 79.31 % which were attributed to the esterification reactions between fatty acids and ethanol [14]. In fact, the concept of blending low viscous pure diesel with the high viscous OMWW biofuel reduces the cost of fuel substantially. The lower cetane value of OMWW biofuel could be balanced by higher cetane value of pure diesel to achieve better combustion.

The biofuel has higher viscosity, higher density, and higher flash point compared to the biofuel blends. The lower calorific value is due to lower hydrogen content in biofuel [37], where the value is about 11.49wt.% [14]. The cetane number of biofuel is slightly lower compared to that of diesel fuel and biofuel blends. However, higher cetane number implies a shorter ignition delay while lower cetane number may produce knock in the engine. Similarly, viscosity and flash point are important properties affecting the volatility, flow of fuel, and spray characteristics. Higher viscosity and flash point leads to lower volatility and consequently poor combustion. Hence it is decided to blend the OMWW biofuel

178 with pure diesel at different proportions to balance most of the properties and to bring it closer to pure  
 179 diesel. Experiments were conducted on CI engine using diesel fuel, OMWW biofuel blends with diesel  
 180 at 10, 20 and 30 percent by volume.

181 **Table 2.** Properties of biofuel, diesel fuel and their blends.

Characteristics	Unit	Diesel	Biofuel	Blends			Test Method
				B30	B20	B10	
Density at 15°C	kg/m <sup>3</sup>	852	899.07	846.75	838.75	832.79	ASTM D1298
Lower calorific value	MJ/kg	43.20	39.21	41.87	42.46	42.91	ASTM D240
Viscosity at 40°C	mPa.s	1.71	10.20	2.58	2.22	1.90	ASTM D445
Flash point	°C	67	117	73	74	77	ASTM D93
Cetane number	-	57.56	54.33	56.63	56.12	57.88	ASTM D613

182

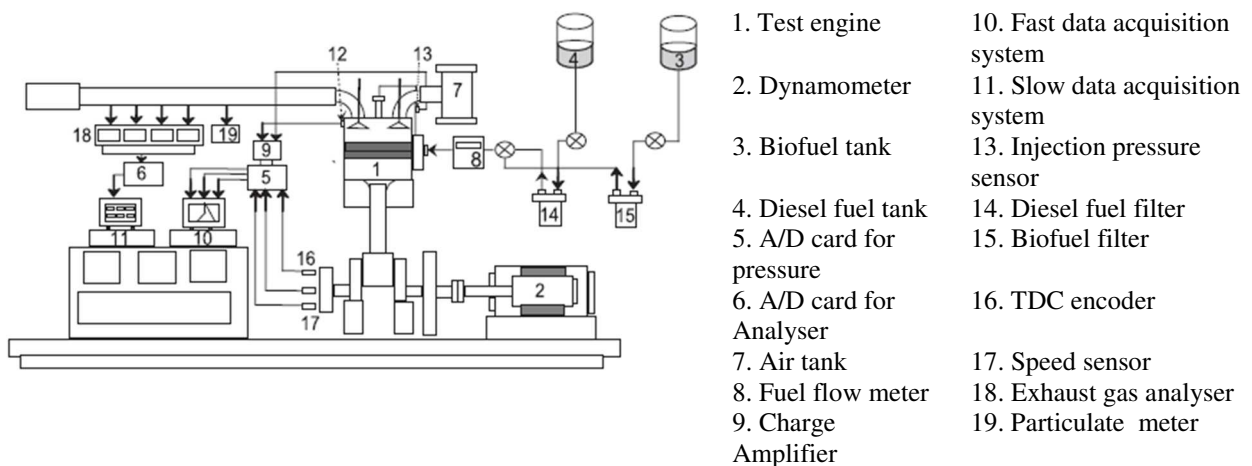
### 183 **2.3. Experimental setup**

184 The results presented in the present study were carried out in the laboratory of IMT  
 185 Atlantique. The experimental test bench is based on a single-cylinder direct injection, naturally  
 186 aspirated, compression ignition engine (manufacturer: LISTER-PETTER). The power output is 4.5  
 187 kW at a rotational speed of 1500 rpm. It is equipped with several instruments to perform the engine  
 188 tests, to analyse the combustion and the measurements of exhaust emissions. The orifice meter  
 189 connected to a large tank is attached to the engine manifold to measure the air flow. The fuel flow rate  
 190 is measured with a Coriolis mass flow meter. Chromel-alumel thermocouple in conjunction with a low  
 191 frequency data acquisition system is used for measuring the exhaust gas temperature. An exhaust  
 192 analyser (COSMA) is used for measuring hydrocarbons (HC) by a flame ionization detector, while  
 193 carbon monoxide (CO) emissions are measured using an infrared device. Nitrogen oxides (NO<sub>x</sub>) in the  
 194 exhaust is measured by using a BECKMAN chemiluminescence NO/NO<sub>x</sub> analyser. Particulate  
 195 emissions are measured using a Pegasor Particle Sensor (PPS-M). PPS-M is based on a novel  
 196 measurement technique enabling real-time, continuous and high sensitivity measurements of raw  
 197 exhausts PM emissions without diluting the exhaust gas. A high frequency data acquisition system in  
 198 connection with two AVL piezoelectric transducers is used for measuring the cylinder pressure and  
 199 fuel line pressure histories. An optical shaft position encoder is used to give signals at TDC. The data  
 200 of cylinder pressure was recorded every 100 consecutive cycles with a sampling interval of about 0.2  
 201 crank angle (CA). Before each experiment, the engine is calibrated according to the manufacturer

202 catalogue values. All data are collected after the engine has stabilised. During the entire investigations,  
 203 the working parameters of the test engine are fixed as injection timing of 13°CA before TDC for,  
 204 engine speed of 1500 rpm, and compression ratio of 18. More details about the acquisition system;  
 205 sensors precision and uncertainty calculation can be found in our previous works [38,39]. Figure 3  
 206 shows the engine experimental setup. A schematic diagram of engine setup is depicted in Figure 4.  
 207 Table 3 shows the engine testing procedure and the engine specifications.



208  
 209 **Fig.3.** Experimental setup.



211 **Fig.4.** Schematic diagram of engine setup.

212

213 **Table 3.** Lister-Petter engine specifications.

General details	Single cylinder, naturally aspirated, 4-Stroke
Cooling system	Air-cooled
Injection system	Compression Ignition, direct injection
Bore×stroke	95.3 mm×88.9 mm
Connecting rod length	165.3 mm
Compression ratio	18:1
displacement volume	630 cm <sup>3</sup>
Fuel injection timing	13° BTDC
Fuel injection pressure	240 bar
Rated power output	4.5 kW at 1500 rpm
Orifices×diameter	4×0.25 mm
Piston type	Cylindrical bowl (diameter : 45mm and depth : 15mm)
IVO	36° CA before TDC
IVC	69° CA after BDC
EVO	76° CA before BDC
EVC	32° CA after TDC

214

215 Before starting the serial tests, the engine test bench was calibrated according to the instructions given  
216 in the manufacturer catalogue. The pressure cylinder, brake torque, flow rates of air, diesel and blend  
217 fuels are registered to determine the engine performance. The injection timing of the pilot fuel is set at  
218 13° CA before TDC for all experiments. Experiments are carried out at a constant speed engine (1500  
219 rpm) and different loads (25%, 50%, 75% and 100% full load).

220

#### 221 **2.4.Combustion analysis model**

222 Processing pressure data in the form of smoothing is essential, depending on the noisy trend of the  
223 pressure signal between successive values. For our case, the smoothing was established using the  
224 smoothing equation of the instantaneous pressure data used by several researchers, as reported in the  
225 literature [40]. The combustion process was examined by the determination of the heat release rate  
226 (HRR). The HRR was calculated analytically by applying the first law of thermodynamics and the  
227 ideal gas equation. As shown in the equation below, to obtain the HRR, the variation of the cylinder  
228 pressure and volume is used.

$$229 \quad \frac{dQ_{net}}{d\theta} = \frac{dQ_c}{d\theta} - \frac{dQ_w}{d\theta} = \frac{\gamma}{\gamma-1} P \left[ \frac{dV}{d\theta} \right] + \frac{1}{\gamma-1} V \left[ \frac{dP}{d\theta} \right] \quad (1)$$

230 Where  $\frac{dQ_{net}}{d\theta}$  is the net HRR,  $\frac{dQ_C}{d\theta}$  is the rate of heat released by the fuel combustion and  $\frac{dQ_w}{d\theta}$  is the  
 231 heat transfer rate through the cylinder wall obtained from the Woschni's correlation [39].  $P$  is the  
 232 cylinder pressure and  $\gamma$  is the ratio of specific heats. From the literature, the  $\gamma$  is generally fixed as  
 233 1.35.  $V$  represents the combustion chamber volume which depends on the crank angle ( $\theta$ ) and the  
 234 geometric parameters of the engine. The cylinder volume  $V$  is obtained as follow:

$$235 \quad V(\theta) = V_d \left[ \frac{Cr}{Cr-1} - \frac{1-\cos\theta}{2} + \frac{1}{2} \sqrt{\left(2\frac{L}{C}\right)^2 - \sin^2\theta} \right] \quad (2)$$

236 Where  $V_d$ ,  $Cr$ ,  $L$  and  $C$  are respectively the displacement volume, the compression ratio, the connecting  
 237 rod length and the stroke.

### 238 **3. Results and discussion**

#### 239 **3.1. Combustion characteristics**

240 In this part, to diagnose the combustion process at different loads, the results of the cylinder pressure  
 241 data, HRR, ignition delay and combustion duration are examined. All the results were compared with  
 242 those of the conventional diesel fuel.

##### 243 **3.1.1. Heat release rate**

244 From the literature, the heat release rate is divided in three steps, ignition delay, premixed combustion  
 245 and diffusion combustion. Fig. 5 shows the evolution of the heat release rate (HRR) versus the crank  
 246 angle (CA) for the tested fuels. The higher peak of HRR for premixed phase is obtained for B0 at  
 247 medium loads and for B20 and B30 at full loads. This is due to the longer ignition delay of B30 and  
 248 B20 in comparison with that of diesel and B10 at high loads, as shown in Fig. 5b. Indeed, we can see  
 249 that the combustion starts earlier for the diesel fuel and for the B10 due to higher density of diesel and  
 250 higher bulk modulus as well as shorter ignition delay [41]. In fact, as reported in the literature, a  
 251 longer ignition delay leads to the accumulation of fuel which burns at higher rate during premixed  
 252 combustion phase leading to higher HRR peak values [39]. However, because of this prolongation of  
 253 the ID, the premixed phase ends later (in the expansion phase) as mentioned previously, at medium  
 254 loads.

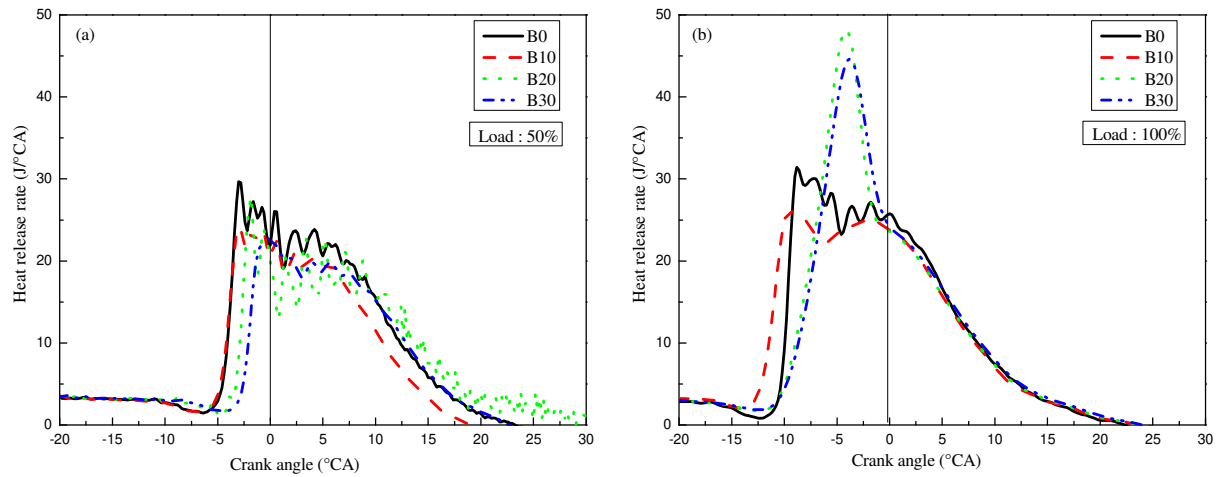


**Fig.5.** Heat release rate (HRR) with crank angle for diesel and diesel-biofuel blend fuels.

255  
256  
257

Moreover, it can be seen from Figure 5 that HRR of diesel is higher than that observed for B10 for all loads studied. According to this Figure 5, the HRR of B10 tends to become similar to that of conventional mode at medium loads, during the ID and the premixed phases. In addition, a separation can be seen in the third phase of HRR. The HRR of diesel remains higher than that of the B10 at premixed and diffusion phases, at the same loads. Furthermore, at full load, the curves are detached at the first and second phases of the HRR and tend to overlap in the diffusion phase. This confirms the results related to ID presented in the next section, where the ID was shorter for the B10 compared to the diesel at full load as shown in Figure 5.

### 3.1.2. Cylinder pressure

Figure 6 presents the evolution of the cylinder pressure at medium and full loads versus crank angle for diesel and biofuel-diesel blend fuels. As shown in Fig 6a, the highest peak of cylinder pressure is observed for B0 (diesel fuel) than that of biofuels tested at medium loads. However, we can explain these behaviors by the difference in energy content of mixed fuels, as mentioned in Table 2. The position of the cylinder pressure peak indicates the speed to release this energy. It is important to mention that the heat release rate depends on the concentration of oxygen contained in fuel (which accelerates combustion), viscosity (which affects atomization and vaporization of fuel) and latent heat (which affects directly the ignition delay and combustion cooling) [42].

273

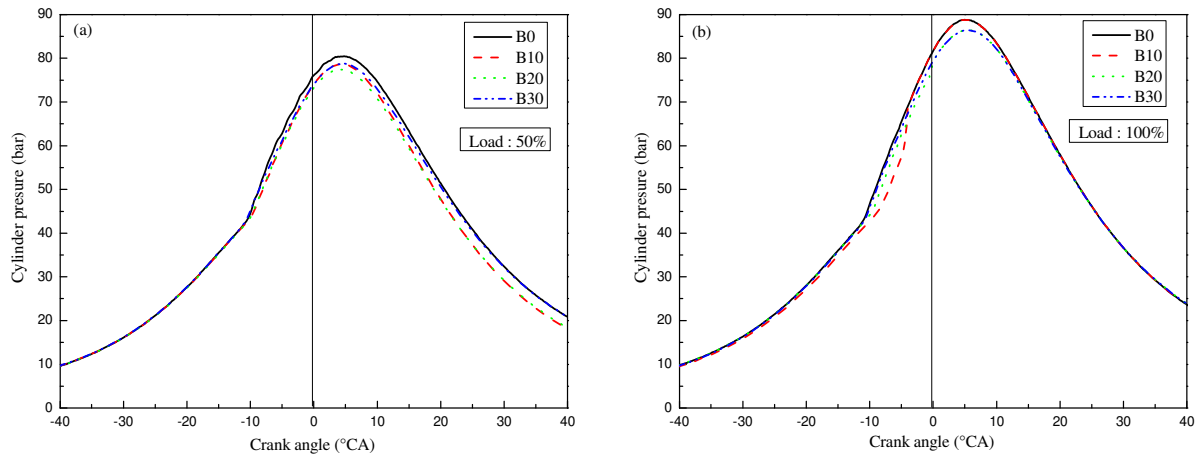


**Fig. 6.** Cylinder pressure variation with crank angle for different biodiesel.

274  
275

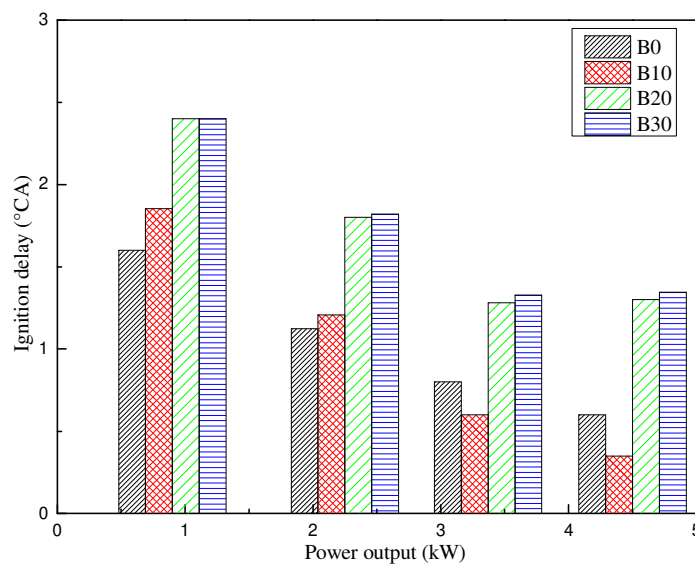
276 The combination of these factors may explain the behavior of the cylinder pressure mentioned in  
 277 Figure 3. In addition, the increase in the concentration of biofuel in the mixture results in a longer  
 278 ignition delay [42]. The combination of the low self-ignition temperature and the relatively high  
 279 cetane number reduce the ignition delay [42]. This can be visualized in Table 2 where we find these  
 280 two parameters for the different mixes studied . Moreover, it can be also seen from this Fig. 6b a  
 281 separation between the curves of cylinder pressure of all the cases studied. This is the consequence of  
 282 a lower heat release rate for B10 and diesel in the premixed combustion (before TDC), as mentioned  
 283 previously, due to the specific heat capacity of B10 and diesel which is higher than that of B20 and  
 284 B30. Furthermore, in the expansion, the curves have the same appearance for all the cases studied and  
 285 overlap perfectly at full load.

286

### 287 3.1.3. Ignition delay

288 The ignition delay (ID) is by definition the interval between the start of injection and the beginning of  
 289 combustion. This parameter is important to analyse correctly the process of combustion and to give  
 290 additional explanations of the behaviour of both the in-cylinder pressure and the rate of heat release.  
 291 From the literature, the ID is composed of two periods. The first one is the physical delay period  
 292 (PDP) and the second one is chemical delay period (CDP). The PDP period is related to the air mixing  
 293 with the fuel atomization, vaporization and decomposition, as reported by Heywood. Regarding the  
 294 CDP, it represents the time required for reaction combustion start.

295 Figure 7 shows the variation of the ignition delay with power output for the fuels tested. The ID  
 296 decreases with increasing the load for all the fuels studied. This can be explained by the elevation of  
 297 the cylinder temperature and pressure as well as the equivalence ratio of the mixture. In addition, it can  
 298 be observed that, for all the cases studied, the ignition delay of B20 and B30 is the highest. This result  
 299 can be explained by the increase in the temperature of the gases in the cylinder which promotes self-  
 300 ignition which reduces the ID of B10 and diesel fuel than that of B20 and B30. Moreover, one can  
 301 observe that at medium and high loads, the ID for B10 tends to be shorter than that of diesel, unlike at  
 302 low loads.



303 **Fig.7.** Ignition delay variation with power output.

304  
 305  
 306 The long ignition delay for B20 and B30 enhances the fuel-air mixture and therefore results in an  
 307 improvement of the premixed combustion phase as discussed previously as illustrated in Figure 5.  
 308 Increasing the concentration of the biofuel in the fuel mixture with diesel accelerates and improves the  
 309 vaporization of the fuel studied. The presence of a significant amount of biofuel also induces a higher  
 310 in cylinder temperature and pressure as shown in Figure 5 and 6.

### 311 3.2. Engine performance

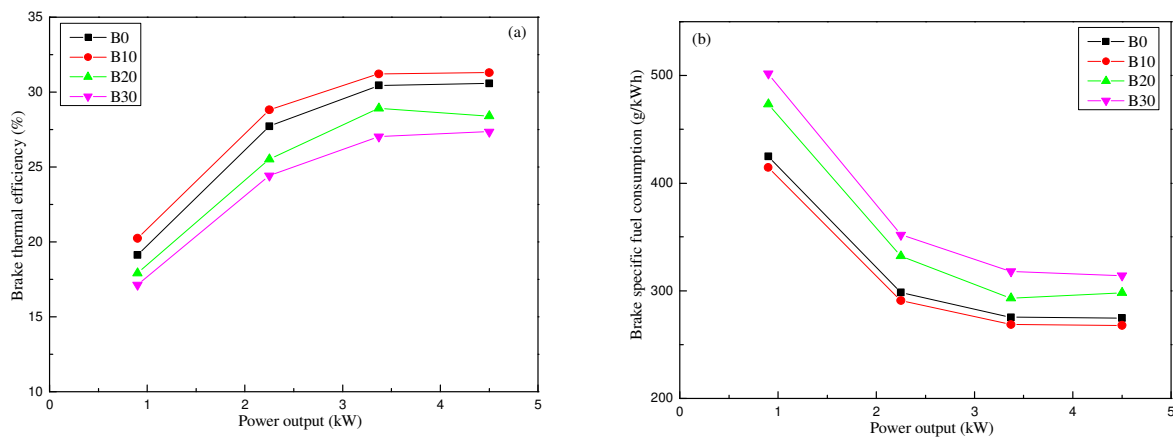
312 To analyze the performance of engine, the brake thermal efficiency (BTE) is examined. It is  
 313 calculated as follow:

$$314 \quad BTE = \frac{P_{out}}{\dot{m}_f LHV_f} \quad (3)$$



315 Where  $P_{out}$  (kW) is the brake power output.  $\dot{m}_f$  is the mass flow rate of fuel (kg/s).

316 It can be seen from Fig. 8a that BTE curves have similar trends for all the fuels over the load  
317 range tested. The thermal efficiency increases as the load increases. This is due to the increase in heat  
318 produced from the combustion inside the cylinder. Moreover, the increase of the equivalence ratio of  
319 the mixture in the cylinder leads to improvement of combustion efficiency. All these factors are  
320 beneficial for increasing BTE. In addition, as shown in Fig. 8a, the BTE increases with a uniform gap  
321 between the curves related to fuels tested.



322 **Fig.8.** Evolution of the BTE (a) and BSFC (b) versus loads.

323 However, according to the Fig. 8a, it is noticed that despite the low calorific value of B10, compared  
324 to that of diesel and the two other blends tested, the performance of B10 remains slightly higher or  
325 similar to that of diesel. On the other hand, the BTE of B10 is the closest to that of Diesel in  
326 comparison to that of B20 and B30. In fact, if biofuel is added in small amount (10%), the biofuel's  
327 high oxygen content induces a good combustion efficiency which results in an improvement in the  
328 brake thermal efficiency (B10). Moreover, this behaviour can be explained by the high cetane number  
329 and flash point as well as a low viscosity than those of B20 and B30 as shown in Table 2. This reflects  
330 the combustion process deterioration of B20 and B30 tested, leading to a reduction of the combustion  
331 efficiency resulting from the low atomization of the fuel tested and of the high viscosity, as reported  
332 by Nour et al. [42]. Consequently, the B30 presents a lower BTE with a value of 28% at full load.  
333 However, for diesel and B20, the BTE is about 31% and 29%, respectively at the same load. The same

334 observation was reported by McCarthy et al [43]. Their study was focused on the analysis and  
335 comparison of performance and emissions of an internal combustion engine fuelled with petroleum  
336 diesel and different biodiesels. They found that the performance of biodiesel fuels reduces with  
337 increasing blend ratio, and the fuel consumption increase was in the range of 7–10%.

338 The Fig. 8b shows the variation of BSFC with respect to load for diesel fuel and diesel-biofuel blends.  
339 Under all load conditions, the BSFC of B20 and B30 is higher of about 14% and 17%, respectively,  
340 compared to that of diesel and B10. This can be explained by the higher viscosity and lower energy  
341 content of B20 and B30 in comparison with that of diesel fuel and B10. This led to injecting higher  
342 quantity of fuel to meet out the same power output as that of pure diesel and B10 operation which  
343 agree with the same observation reported in literature [43,44].

344

### 345 **3.3. Exhaust emissions**

#### 346 ***3.3.1. HC and CO emissions***

347 The emissions of unburned hydrocarbons (HC) are by definition the result of incomplete fuel  
348 combustion. Fig. 9a shows the variation of the HC emissions versus loads. It can be noticed that the  
349 curves have the same trend. At low loads, the concentration of HC emissions tends to be the same. At  
350 high loads, the B10 emits less HC than the other cases studied, with a maximum observed for the case  
351 of B20. These observations are attributed to the prolonged ID and the delayed combustion into the  
352 expansion stroke end. All these parameters will induce a less time of high temperature to give  
353 complete conversion, consequently, a high concentration of HC emissions as reported by Nour et al.  
354 [42].

355 The variation of the concentration of carbon monoxide (CO) emissions recorded in the exhaust  
356 gases for the different fuels tested is shown in Fig.9b. It can be seen that the curves describe the same  
357 trend regardless of the fuel studied. Furthermore, the concentration of CO emissions increases mainly  
358 at high load due to high amount of fuel injected and less available oxygen for complete combustion of  
359 the fuel. The same observation was reported in literature [42,45].

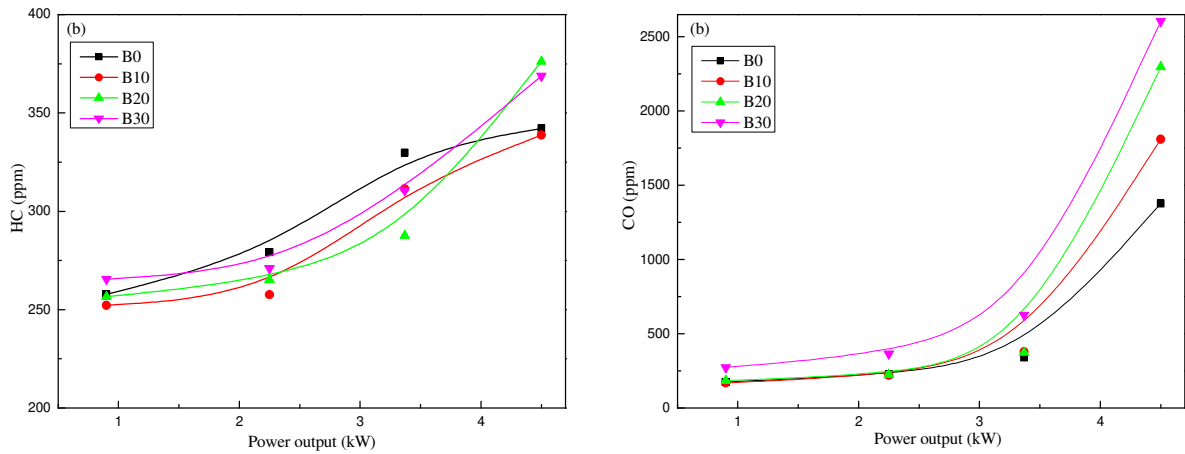


**Fig.9.** Variation of HC emissions (a) and CO emissions (b) versus loads.

360  
361

362 At low and medium loads, the concentration of CO emissions remains mostly the same for diesel, B10  
363 and B20. In addition, at high load, the diesel was the less pollutant fuel in terms of CO emissions.  
364 Regarding the case of B30 blend, it had a maximum of CO emissions regardless the load studied. This  
365 can be explained by the formation of large droplet size, worsening fuel atomization and the highest  
366 viscosity of fuel.

### 367 3.3.2. *NOx and particulate emissions*

368 For many years, it has been known that the major problem of the conventional diesel engine is  
369 the high concentration of particulate and NOx emissions [38]. In this part, the concentration  
370 of this emission type was analysed. The results obtained from the combustion of the different  
371 fuels (diesel and diesel-biofuel blends) are depicted in Figure 10.

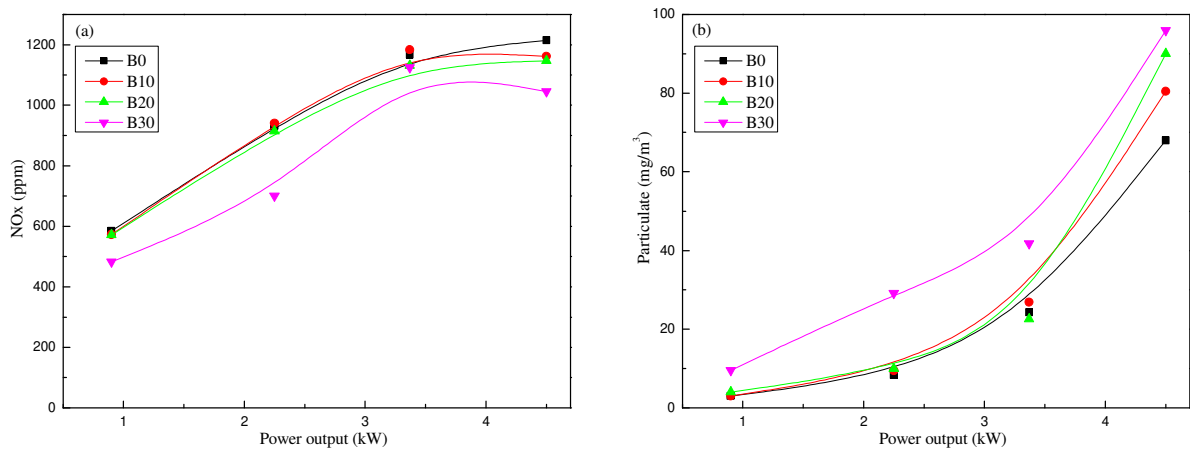


**Fig.10.** Variation of NOx emissions (a) and particulates emissions (b) versus loads.

372

373 The analysis of NO<sub>x</sub> emissions in exhaust gases at different loads is shown in Fig. 10a. It can be  
374 perceived that the curves describe the same trend regardless the fuel studied. Moreover, the  
375 concentration of NO<sub>x</sub> emissions remains similar to that of diesel fuel for all loads except for the B30  
376 fuel. This confirms the results previously presented in Fig. 10b, where CO emissions are inversely  
377 proportional to NO<sub>x</sub> emissions. This behaviour was also reported by Heywood [46]. This is the  
378 consequence of the decrease of the average gas temperature in the cylinder.

379 According to the literature, the early formation of soot particles at the diffusion combustion process  
380 level is due to the dissociation of the fuel at high temperature [46]. One of the main factors in the  
381 formation of these emissions is the biofuel tested composition. In fact, the bond C-C strongly  
382 favouring the production of these emissions [46].

383 From Fig. 10b, it was found that the concentrations of soot emissions were similar at low and medium  
384 loads except for B30, where it has the highest concentration of soot emissions whatever the load  
385 studied. Moreover, regarding the full load, B10 and B20 remain more pollutant than diesel in terms of  
386 soot emissions. Alagu et al [34] had reported the same results. They found that at full load condition,  
387 the concentration of soot emissions of biodiesel (B10 blend) was higher (52.8%) than fossil diesel  
388 operation. This is due to the highest viscosity of fuel leading to worsening fuel atomization resulting in  
389 the formation of large droplet size. Moreover, a lower cetane number produces a longer ID which  
390 induces to short time for the formed soot to be oxidized, consequently an increase of soot emissions  
391 [42].

#### 392 **4. Conclusion**

393 This study focused on the impact of OMWW biofuel blended with diesel fuel on performance,  
394 combustion and pollutant emissions of a compression ignition engine. Engine tests were performed  
395 with different proportions of biofuel.

396 From the present results, the blend of B10 presents a reduction of 26% of carbon monoxide, 12% of  
397 unburned hydrocarbons and 12% of particle emissions with an improvement in brake thermal  
398 efficiency of 10% compared to those of B20. At medium loads, B30 had a higher carbon monoxide  
399 concentration and particulate emissions of about 65% and 55%, respectively, with a deterioration of  
400 the brake thermal efficiency of 13% compared to that of B10. On the other hand, at high loads, B10

401 has less polluting effects by around 43% of carbon monoxide, 10% of unburned hydrocarbons and  
402 20% of particles compared to that of B30. Consequently, B10 is the cleaner and more efficient fuel  
403 than B20 and B30. Furthermore, it should be noted that despite the degradation of the performance of  
404 B20 and B30, these biofuels make it possible to obtain acceptable results while being partly composed  
405 of biofuel from waste. This will therefore allow to replace fossil diesel fuel and help to reduce  
406 greenhouse gas emissions.

407 On the other hand, to reduce the economic impact caused by the fossil fuel crisis and avoid  
408 relying on existing biofuels, it is important to seek locally available and renewable biofuel. Wherefore,  
409 OMWW biofuel has a high potential to be used as engine fuel for reducing greenhouse gas emissions.  
410 A future work will be devoted to the production of biofuel from OMWW using methanol as solvent.  
411 Engine tests will be carried out using different mixtures and results will be compared to the present  
412 work.

## 413 **5. Acknowledgments**

414 The authors are very grateful to the technicians of the Energy Systems and Environment  
415 Department of IMT Atlantique for their advice and support.

## 416 **6. References**

- 417
- 418 [1] Agarwal AK, Das LM. Biodiesel development and characterization for use as a fuel in  
419 compression ignition engines. *J Eng Gas Turbines Power* 2001;123:440.  
420 doi:10.1115/1.1364522.
- 421 [2] Fahmi I, Cremaschi S. Process synthesis of biodiesel production plant using artificial  
422 neural networks as the surrogate models. *Comput Chem Eng* 2012;46:105–23.  
423 doi:10.1016/j.compchemeng.2012.06.006.
- 424 [3] Marcilla A, Catalá L, Valdés FJ, Hernández MR. A review of thermochemical  
425 conversion of microalgae. *Renew Sustain Energy Rev* 2013;27:11–9.  
426 doi:10.1016/j.rser.2013.06.032.
- 427 [4] García-Martín JF, Barrios CC, Alés-Álvarez FJ, Dominguez-Sáez A, Alvarez-Mateos  
428 P. Biodiesel production from waste cooking oil in an oscillatory flow reactor.  
429 Performance as a fuel on a TDI diesel engine. *Renew Energy* 2018;125:546–56.  
430 doi:10.1016/j.renene.2018.03.002.
- 431 [5] Demirbas A. Political, economic and environmental impacts of biofuels: A review.

- 432 Appl Energy 2009;86:108–17. doi:10.1016/j.apenergy.2009.04.036.
- 433 [6] De Vries SC, van de Ven GWJ, van Ittersum MK. First or second generation biofuel  
434 crops in Brandenburg, Germany? A model-based comparison of their production-  
435 ecological sustainability. Eur J Agron 2014;52:166–79. doi:10.1016/j.eja.2013.09.012.
- 436 [7] Naik SN, Goud V V., Rout PK, Dalai AK. Production of first and second generation  
437 biofuels: A comprehensive review. Renew Sustain Energy Rev 2010;14:578–97.  
438 doi:10.1016/j.rser.2009.10.003.
- 439 [8] Masera K, Hossain AK. Biofuels and thermal barrier: A review on compression  
440 ignition engine performance, combustion and exhaust gas emission. J Energy Inst  
441 2018. doi:10.1016/j.joei.2018.02.005.
- 442 [9] Gollakota ARK, Kishore N, Gu S. A review on hydrothermal liquefaction of biomass.  
443 Renew Sustain Energy Rev 2018;81:1378–92. doi:10.1016/j.rser.2017.05.178.
- 444 [10] Srirangan K, Akawi L, Moo-Young M, Chou CP. Towards sustainable production of  
445 clean energy carriers from biomass resources. Appl Energy 2012;100:172–86.  
446 doi:10.1016/j.apenergy.2012.05.012.
- 447 [11] Bridgwater, A.V., Boocock DGB. Developments in Thermochemical Biomass  
448 Conversion. Springer S. Springer Science & Business Media; 2013.
- 449 [12] Ben Rahal N, Barba FJ, Barth D, Chevalot I. Supercritical CO<sub>2</sub> extraction of oil, fatty  
450 acids and flavonolignans from milk thistle seeds: Evaluation of their antioxidant and  
451 cytotoxic activities in Caco-2 cells. Food Chem Toxicol 2015;83:275–82.  
452 doi:10.1016/j.fct.2015.07.006.
- 453 [13] Hadhoum, L., Loubar, K., Paraschiv, M., Burnens, G., Awad, S & Tazerout M.  
454 Optimization of oleaginous seeds liquefaction using response surface methodology.  
455 Biomass Convers Biorefinery 2020.
- 456 [14] Hadhoum L, Burnens G, Loubar K, Balistrrou M, Tazerout M. Bio-oil recovery from  
457 olive mill wastewater in sub-/supercritical alcohol-water system. Fuel 2019;252:360–  
458 70. doi:10.1016/j.fuel.2019.04.133.
- 459 [15] Wastewater OM, Tsagaraki E, Lazarides HN, Petrotos KB. Olive mill wastewater  
460 treatment. Util. By-products Treat. Waste Food Ind., Springer, Boston, MA; 2004, p.  
461 133–57. doi:10.1007/978-0-387-35766-9\_8.
- 462 [16] Jeguirim M, Chouchène A, Favre-Réguillon A, Trouvé G, Le Buzit G. A new  
463 valorisation strategy of olive mill wastewater: Impregnation on sawdust and  
464 combustion. Resour Conserv Recycl 2012;59:4–8.  
465 doi:10.1016/j.resconrec.2011.03.006.
- 466 [17] Kraiem N, Jeguirim M, Limousy L, Lajili M, Dorge S, Michelin L, et al. Impregnation  
467 of olive mill wastewater on dry biomasses: Impact on chemical properties and  
468 combustion performances. Energy 2014;78:479–89. doi:10.1016/j.energy.2014.10.035.
- 469 [18] Hadhoum L, Balistrrou M, Burnens G, Loubar K, Tazerout M. Hydrothermal  
470 liquefaction of oil mill wastewater for bio-oil production in subcritical conditions.  
471 Bioresour Technol 2016;218. doi:10.1016/j.biortech.2016.06.054.

- 472 [19] Sierra J, Martí E, Montserrat G, Cruaáas R, Garau MA. Characterisation and evolution  
473 of a soil affected by olive oil mill wastewater disposal. *Sci Total Environ*  
474 2001;279:207–14. doi:10.1016/S0048-9697(01)00783-5.
- 475 [20] Vitolo S, Petarca L, Bresci B. Treatment of olive oil industry wastes. *Bioresour*  
476 *Technol* 1999;67:129–37. doi:10.1016/S0960-8524(98)00110-2.
- 477 [21] Hadhoum L, Balistrrou M, Burnens G, Loubar K, Tazerout M. Hydrothermal  
478 liquefaction of oil mill wastewater for bio-oil production in subcritical conditions.  
479 *Bioresour Technol* 2016;218:9–17. doi:10.1016/j.biortech.2016.06.054.
- 480 [22] Miranda T, Esteban A, Rojas S, Montero I, Ruiz A. Combustion analysis of different  
481 olive residues. *Int J Mol Sci* 2008;9:512–25. doi:10.3390/ijms9040512.
- 482 [23] Kipçak E, Söğüt OÖ, Akgün M. Hydrothermal gasification of olive mill wastewater as  
483 a biomass source in supercritical water. *J Supercrit Fluids* 2011;57:50–7.  
484 doi:10.1016/j.supflu.2011.02.006.
- 485 [24] Poerschmann J, Baskyr I, Weiner B, Koehler R, Wedwitschka H, Kopinke FD.  
486 Hydrothermal carbonization of olive mill wastewater. *Bioresour Technol*  
487 2013;133:581–8. doi:10.1016/j.biortech.2013.01.154.
- 488 [25] Khiari K, Tarabet L, Awad S, Loubar K, Mahmoud R, Tazerout M. Optimization of  
489 Pistacia lentiscus oil transesterification process using central composite design. *Waste*  
490 *and Biomass Valorization* 2018;0:0. doi:10.1007/s12649-018-0257-2.
- 491 [26] Şen M, Emiroğlu AO, Keskin A. Production of biodiesel from broiler chicken  
492 rendering fat and investigation of its effects on combustion, performance, and  
493 emissions of a diesel engine. *Energy & Fuels* 2018;acs.energyfuels.8b00278.  
494 doi:10.1021/acs.energyfuels.8b00278.
- 495 [27] Harreh D, Saleh AA, Reddy ANR, Hamdan S. An experimental investigation of  
496 karanja Biodiesel production in Sarawak, Malaysia. *J Eng (United States)* 2018;2018.  
497 doi:10.1155/2018/4174205.
- 498 [28] Tarabet L, Loubar K, Lounici MS, Hanchi S, Tazerout M. Eucalyptus biodiesel as an  
499 alternative to diesel fuel: Preparation and tests on di diesel engine. *J Biomed*  
500 *Biotechnol* 2012;2012. doi:10.1155/2012/235485.
- 501 [29] Agarwal AK. Biofuels (alcohols and biodiesel) applications as fuels for internal  
502 combustion engines. *Prog Energy Combust Sci* 2007;33:233–71.  
503 doi:10.1016/j.pecs.2006.08.003.
- 504 [30] Suresh M, Jawahar CP, Richard A. A review on biodiesel production , combustion ,  
505 performance , and emission characteristics of non-edible oils in variable compression  
506 ratio diesel engine using biodiesel and its blends. *Renew Sustain Energy Rev*  
507 2018;92:38–49. doi:10.1016/j.rser.2018.04.048.
- 508 [31] Indrareddy N, Venkateswarlu K, Konijeti R. Experimental investigation of algae  
509 biofuel–diesel blends on performance of a CRDI diesel engine. *Int J Ambient Energy*  
510 2020;0:1–17. doi:10.1080/01430750.2020.1725630.
- 511 [32] Miraculas GA, Bose N, Raj RE. Optimization of biofuel blends and compression ratio  
512 of a diesel engine fueled with calophyllum inophyllum oil methyl ester. *Arab J Sci Eng*

- 513 2016;41:1723–33. doi:10.1007/s13369-015-1942-0.
- 514 [33] Chauhan BS, Singh RK, Cho HM, Lim HC. Practice of diesel fuel blends using  
515 alternative fuels: A review. *Renew Sustain Energy Rev* 2016;59:1358–68.  
516 doi:10.1016/j.rser.2016.01.062.
- 517 [34] Alagu RM, Sundaram EG. Preparation and characterization of pyrolytic oil through  
518 pyrolysis of neem seed and study of performance , combustion and emission  
519 characteristics in CI engine. *J Energy Inst* 2018;91:100–9.  
520 doi:10.1016/j.joei.2016.10.003.
- 521 [35] Khiari, K., Tarabet, L., Awad, S., Loubar, K., Mahmoud, R., Tazerout, M & Derradji  
522 M. Optimization of bio-oil production from Pistacia lentiscus seed liquefaction and its  
523 effect on diesel engine performance and pollutant emissions. *Biomass Convers*  
524 *Biorefinery* 2020:1–14.
- 525 [36] Hadhoum L, Balistrrou M, Burnens G, Loubar K, Tazerout M. Hydrothermal  
526 liquefaction of oil mill wastewater for bio-oil production in subcritical conditions.  
527 *Bioresour Technol* 2016;218:9–17. doi:10.1016/j.biortech.2016.06.054.
- 528 [37] Hossain AK, Davies PA. Plant oils as fuels for compression ignition engines: A  
529 technical review and life-cycle analysis. *Renew Energy* 2010;35:1–13.  
530 doi:10.1016/j.renene.2009.05.009.
- 531 [38] Aklouche FZ, Loubar K, Bentebbiche A, Awad S, Tazerout M. Predictive model of the  
532 diesel engine operating in dual-fuel mode fuelled with different gaseous fuels. *Fuel*  
533 2018;220:599–606. doi:10.1016/j.fuel.2018.02.053.
- 534 [39] Aklouche FZ, Loubar K, Bentebbiche A, Awad S, Tazerout M. Experimental  
535 investigation of the equivalence ratio influence on combustion, performance and  
536 exhaust emissions of a dual fuel diesel engine operating on synthetic biogas fuel.  
537 *Energy Convers Manag* 2017;152:291–9. doi:10.1016/j.enconman.2017.09.050.
- 538 [40] Bora BJ, Saha UK, Chatterjee S, Veer V. Effect of compression ratio on performance,  
539 combustion and emission characteristics of a dual fuel diesel engine run on raw biogas.  
540 *Energy Convers Manag* 2014;87:1000–9. doi:10.1016/j.enconman.2014.07.080.
- 541 [41] Gumus M. A comprehensive experimental investigation of combustion and heat release  
542 characteristics of a biodiesel (hazelnut kernel oil methyl ester) fueled direct injection  
543 compression ignition engine. *Fuel* 2010;89:2802–14. doi:10.1016/j.fuel.2010.01.035.
- 544 [42] Nour M, Attia AMA, Nada SA. Combustion, performance and emission analysis of  
545 diesel engine fuelled by higher alcohols (butanol, octanol and heptanol)/diesel blends.  
546 *Energy Convers Manag* 2019;185:313–29. doi:10.1016/j.enconman.2019.01.105.
- 547 [43] Mccarthy P, Rasul MG, Moazzem S. Analysis and comparison of performance and  
548 emissions of an internal combustion engine fuelled with petroleum diesel and different  
549 bio-diesels. *Fuel* 2011;90:2147–57. doi:10.1016/j.fuel.2011.02.010.
- 550 [44] Muralidharan K, Vasudevan D. Performance , emission and combustion characteristics  
551 of a variable compression ratio engine using methyl esters of waste cooking oil and  
552 diesel blends. *Appl Energy* 2011;88:3959–68. doi:10.1016/j.apenergy.2011.04.014.
- 553 [45] Ashraful AM, Masjuki HH, Kalam MA, Fattah IMR, Imtenan S, Shahir SA, et al.



- 554 Production and comparison of fuel properties , engine performance , and emission  
555 characteristics of biodiesel from various non-edible vegetable oils : A review. Energy  
556 Convers Manag 2014;80:202–28. doi:10.1016/j.enconman.2014.01.037.
- 557 [46] Yorobiev Ya. I, Zharnov VM, Naumenko VD. Internal combustion engine. vol. 21.  
558 1985.
- 559

# Graphical abstract

